

Degradation of III–V Quantum Dot Lasers Grown Directly on Silicon Substrates

Samuel Shutts , Craig P. Allford , Clemens Spinnler, Zhibo Li, Angela Sobiesierski, Mingchu Tang , Huiyun Liu , and Peter M. Smowton

Abstract—Initial age-related degradation mechanisms for InAs quantum dot lasers grown on silicon substrates emitting at 1.3 μm are investigated. The rate of degradation is observed to increase for devices operated at higher carrier densities and is therefore dependent on gain requirement or cavity length. While carrier localization in quantum dots minimizes degradation, an increase in the number of defects in the early stages of aging can increase the internal optical-loss that can initiate rapid degradation of laser performance due to the rise in threshold carrier density. Population of the two-dimensional states is considered the major factor for determining the rate of degradation, which can be significant for lasers requiring high threshold carrier densities. This is demonstrated by operating lasers of different cavity lengths with a constant current and measuring the change in threshold current at regular intervals. A segmented-contact device, which can be used to measure the modal absorption and also operate as a laser, is used to determine how the internal optical-loss changes in the early stages of degradation. Structures grown on silicon show an increase in internal optical loss, whereas the same structure grown on GaAs shows no signs of increase in internal optical loss when operated under the same conditions.

Index Terms—Quantum dots, semiconductor defects, semiconductor laser.

I. INTRODUCTION

THE direct growth of III-V semiconductors on silicon and the demonstration of long-lived devices from such materials has become one of the most pressing concerns in semiconductor science. Building on the pioneering work of the Bhattacharya group, in showing such an approach is feasible [1], it is now of much interest because of the need for on-chip optical sources for Silicon Photonics and ultimately for combining electronics and photonics. Furthermore, significantly larger wafer sizes should be possible for III-Vs grown on silicon, than with

the native substrates, due to the superior mechanical strength of silicon. Such an increase in wafer size is expected to yield a reduction in manufacturing cost at the component level. Mismatched growth on non-native substrates gives rise to a higher defect density due to lattice mismatch and differences in thermal expansion coefficient. For GaAs and Si, the difference is 4% and 120% respectively. Inevitably, a higher defect density has deleterious effects on device performance and increases the rate of age-related degradation. For the polar III-V semiconductors grown on a non-polar Si substrate it is also necessary to minimize defects created by anti-phase domains. This latter problem has largely been solved, and high quality devices produced, through the use of offcut Si substrates and the subsequent growth of effectively 2-dimensional AlAs layers [2], the use of GaAs on v-grooved template (GoVS) on exactly (001) orientated Si [3] or the use of thin GaP nucleation layers on (001) Si [4], [5].

For GaAs grown directly on Si, the number of threading dislocations falls with distance from the interface, as described by a power law [6], and several microns of growth can therefore be used as a ‘buffer’ to reduce the number of defects to a level satisfactory for subsequent deposition of active III-V layers. However, this approach leads to thick epitaxial layers which can cause wafer bowing or thermal cracks because of the thermal expansion mismatch with the underlying silicon substrate. To enhance the removal of threading dislocations (TDs), there has been much success from incorporating dislocation filter layers (DFL)s. These DFLs consist of strained layer superlattices, which due to a large strain-thickness product, encourage in-plane movement of TDs causing them to either meet and annihilate or terminate at the wafers edge. The advantage of DFLs is that they reduce the total thickness of III-V material which needs to be deposited in order to obtain an acceptable level of defects, and this alleviates strain-induced wafer-bow and thermal cracking. Incorporating multiple defect filter layers, combined with in-situ thermal annealing during growth, has shown to dramatically reduce the threshold current of III-V lasers on Si and, with relevance for the work presented later, to cause an increase in the lasing wavelength [7]. Devices have recently been demonstrated with performance which is competitive to those grown on native substrates [2], [8]–[10] and extended to InAs dots on InP on Si and lasers emitting in the 1.55 μm wavelength range [11].

Attention has now turned to the reliability and the degradation processes in these lasers [12]. It is understood that both the number and size of defects present in the laser structure can increase during operation and this in-turn degrades performance,

Manuscript received February 20, 2019; revised April 6, 2019; accepted April 30, 2019. Date of publication May 10, 2019; date of current version June 24, 2019. This work was funded by the Engineering and Physical Sciences Research Council under Grant EP/P006973/1. (Corresponding author: Samuel Shutts.)

S. Shutts, C. P. Allford, Z. Li, A. Sobiesierski, and P. M. Smowton are with the School of Physics and Astronomy, Cardiff University, Cardiff CF10 3AT, U.K. (e-mail: shuttss@cardiff.ac.uk; allfordcp1@cardiff.ac.uk; LiZ74@cardiff.ac.uk; kestlea@cardiff.ac.uk; smowtonpm@cardiff.ac.uk).

C. Spinnler is with the University of Basel, 4001 Basel, Switzerland (e-mail: c.spinnler@unibas.ch).

M. Tang and H. Liu are with the Department of Electronic and Electrical Engineering, University College London, London WC1E 6BT, U.K. (e-mail: mingchu.tang.11@ucl.ac.uk; huiyun.liu@ucl.ac.uk).

Color versions of one or more of the figures in this paper are available online at <http://ieeexplore.ieee.org>.

Digital Object Identifier 10.1109/JSTQE.2019.2915994

the extent of which impacts overall life-time of the device. Initial reports of degradation studies carried out with InAs/GaAs quantum dot (QD) laser structures grown on Ge-on-Si 'virtual' substrates revealed extrapolated lifetimes (doubling of threshold current) exceeding 4600 hours, significantly out performing lasers with quantum well (QW) active regions also grown on Si [13], [14]. This significant result was predicted and has been attributed to two major advantages of using QDs. Firstly, they can effectively deflect defects or pin them preventing loop formation, and secondly, they can localise charge carriers preventing them from diffusing laterally and recombining non-radiatively at a defect site. The latter reduces the rate of degradation because it suppresses recombination enhanced defect reactions (REDR) [15], a process which can cause dislocation climb, increasing non-radiative recombination and potentially, optical mode loss. With QW active regions, carriers are able to diffuse in the plane of the well and therefore capture into a defect state is more probable. This lack of carrier localization compared to QDs, combined with the inability to effectively deflect dislocations, means QW lasers grown on Si substrates experience very short lifetimes [14], [16]. However, it is important to note that the quantum dots used in laser structures are populated via bulk and 2-dimensional states and carrier localisation only occurs if the majority of the carriers populate the localised quantum dot states and not the extended states. A detailed study of the effective diffusion length of carriers in the composite quantum dot/2-dimensional (2D) state system [17] shows that at low injection level, which is a measure of carrier density and achieved at threshold and above using e.g., long lasers, the diffusion length is very low $\sim 0.75 \mu\text{m}$ corresponding to a regime when carriers are captured quickly and localised in the dots. As the gain requirement and the injection level is increased, by using shorter lasers, the diffusion length increases to $\sim 1.5 \mu\text{m}$ as carriers of at least one carrier type populate the 2D states. This analysis suggests that we might expect the degradation rate in quantum dot lasers to be related to the carrier density at threshold, which is itself related to the gain requirement or total optical loss. Recent measurements [18] have shown that the degradation rate is lower in p-modulation doped quantum dot lasers grown on silicon and in this case the electron and hole quasi-Fermi levels are both moved towards the valence states [19] reducing the electron population able to access the 2D states, also supporting the argument that the carrier density populating the extended states, and thus able to access the defects, is critical in addition to the number of defects present.

In this study, we examine the early stage degradation of quantum dot lasers to better understand how quantum dots are reducing degradation and to understand how to maximise the effectiveness of these processes. Long-term reliability studies for devices following these approaches will be the focus of further work.

II. GROWTH STRUCTURE AND FABRICATION

We made use of the well-established InAs/GaAs QD material system, emitting from $1.2 - 1.3 \mu\text{m}$, where much effort has been made to overcome the challenges of growing III-Vs on Si.

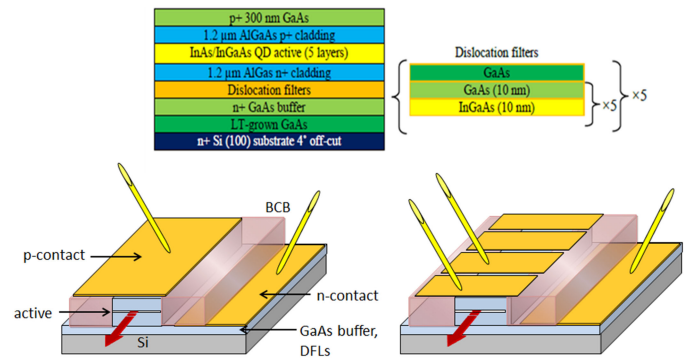


Fig. 1. (a) Schema of epitaxial growth structure including details of defect filters and (b) ridge-waveguide on Si substrate laser (left) and segmented contact test structure (right).

The epitaxial structure, illustrated schematically in Fig. 1a, was grown on a (001) – orientated n-doped Si substrate with 4° off-cut towards $\langle 110 \rangle$, and formed using solid-source molecular beam epitaxy (MBE). Here, for simplicity, the III-V materials are grown over the entire Si wafer, although for eventual application we envisage selective area growth of the III-Vs in recessed areas over only part of the wafer, which will limit the stress leading to wafer bow. The active region contained five InAs/InGaAs dot-in-well (DWELL) structures with 50 nm GaAs spacer layers between them. The rest of the waveguide was formed by $\text{Al}_{0.40}\text{Ga}_{0.60}\text{As}$ cladding layers. Before the active III-V structure was formed, a low temperature (LT) grown GaAs layer was deposited, followed by a 1 micron thick buffer layer and five DFLs. The total thickness of these intermediate layers was $\sim 2.8 \mu\text{m}$. A comparator sample grown on GaAs (used to measure the internal loss as function of aging), has nominally the same structure as that grown on Si, but without the defect filter layers and thick GaAs buffer layer.

Ridge waveguides, shown schematically in Fig. 1b were dry-etched to a depth of approximately $3.2 \mu\text{m}$ using an Oxford Instruments Plasmalab 100. The epi-side n-contact (AuGe/Ni/Au) was deposited and annealed prior to planarising with Benzocyclobutene (BCB) and later re-exposed by back-etching the BCB using reactive ion etching (RIE) with a CF_4/O_2 plasma before final curing at 300°C . Cr/Au was deposited for the p-contact to a thickness of 10 and 400 nm respectively. Test structures to evaluate the optical loss, using the segmented contact method [20], are fabricated in a similar manner except that the top p-contact and underlying GaAs contact layer are etched to leave $4 \mu\text{m}$ wide gaps between contacts formed on a $300 \mu\text{m}$ pitch. These test structures can also be operated as a laser by driving all the sections in forward bias.

Cleaved-facet Fabry-Perot devices are produced by first thinning the Si substrate by lapping. The facets are uncoated. Samples are mounted on T08 transistor headers epi-side up using a silver-loaded epoxy resin and each laser is wire bonded using $30 \mu\text{m}$ aluminum wires. It is appreciated that this method of mounting is not optimized for heat extraction and therefore limits the performance of the devices when operating CW but will be sufficient for our studies of the near-term degradation processes.

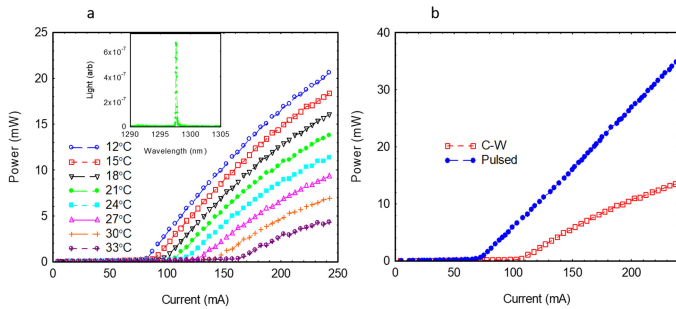


Fig. 2. (a) Power-current characteristics vs. temperature for a $10 \mu\text{m} \times 3 \text{ mm}$ laser operating CW. Inset: shows lasing wavelength at 21°C and at 10% above threshold current. (b) Power-current curves for $10 \mu\text{m} \times 3 \text{ mm}$ laser operated pulsed (solid symbols) and CW (open symbols).

The power-current (P-I) characteristics for a typical $10 \mu\text{m} \times 3 \text{ mm}$ CW operated laser are shown in Fig. 2a as a function of temperature. The inset shows the lasing wavelength measured 10% above threshold at 21°C and has a peak value of 1297 nm. There is a characteristic thermal roll-over in the power level as the current is increased and this is evident when we compare it to the device run pulsed at the same heat-sink temperature, as illustrated in Fig. 2b. The pulsed devices are run at a frequency of 1 kHz and a pulse length of 1000 ns and these values are chosen such that small increases in frequency or duration make no observable difference to threshold current or power output. We therefore believe the generation of heat during pulsed operation is having a negligible effect on operation. As expected, there is an increase in threshold current in CW operation due to the effects of self-heating, which is caused by the resistance of metal-semiconductor contact and the diode junction, i.e., via joule-heating. When performing CW measurements, there is a finite amount of time for self-heating to take full effect as the current increases and therefore the P-I data was taken in a quasi-steady state with a step rate of $\sim 1.4 \text{ mA s}^{-1}$. The difference of the active temperature of the laser relative to the heat-sink can be estimated by comparing pulsed and CW threshold current densities. The temperature difference was measured to be between 10 and 15°C (for a heat sink temperature of 21°C), with less than 5°C variation from shortest and longest cavities. This small difference in temperature between devices of different cavity length, minimises the likelihood that devices will experience different rates of degradation due to temperature variations.

III. RELIABILITY TESTING: RESULTS AND DISCUSSION

Due to the different threshold gain requirement, lasers with different cavity lengths exhibit different characteristics such as, threshold carrier density, operating wavelength, external differential efficiency and current-voltage dependence and we expect they may also have different degradation rates due to the different threshold carrier density. Lasers were tested with cavity lengths of 2, 3 and 4 mm. Each device was operated CW at a constant current (1.3 times initial threshold) and a temperature of 21°C , with the light output, voltage and temperature monitored at 5 minute intervals. Testing was only interrupted to

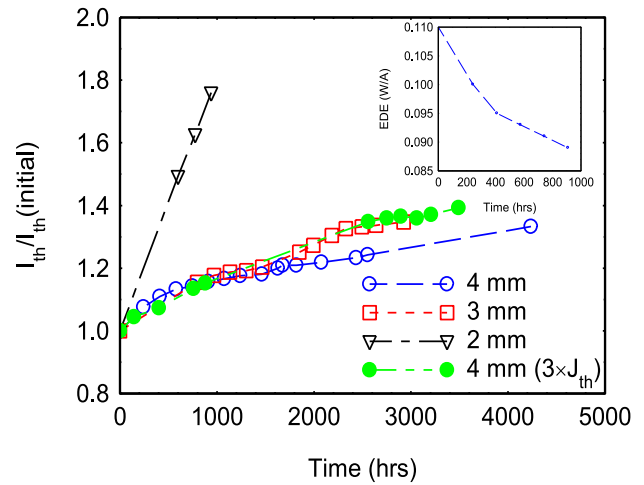


Fig. 3. Threshold current density (J_{th}) versus CW operating time for lasers of different cavity length, at 21°C . Inset showing external differential efficiency (EDE) vs. time for a 4 mm long laser aged at 1.3 times initial threshold and 21°C .

perform light-current-voltage (L-I-V) and wavelength measurements. The experiment revealed a reduction in the light output for lasers of all cavity lengths, with degradation occurring more rapidly for lasers with shorter cavity lengths (a greater fractional loss in light output with time). Threshold current values (J_{th}) extracted from interval L-I measurements, plotted in Fig. 3, show an increase in threshold current with aging, which is significant for the shortest (2 mm) laser which failed to operate CW beyond 1000 hours. As aging proceeds, the external differential efficiency of the lasers also reduced, with the most significant fall occurring within the first few hundred hours of operation, as shown in the inset of Fig. 3 for a 4 mm long laser. Another 4 mm laser was operated at 3.0 times threshold to observe how the increase in current density, for a given cavity length, would affect degradation rate. We note that the current density used is the same as for the 2 mm long laser that degraded rapidly. Operation at increased current density is known to affect long term degradation rate of diode lasers but here we look for the relative size of effects in lasers of different length and hence optical loss. Above threshold the carrier density does not increase in proportion to the current density because of the enhanced stimulated emission rate in the lower loss (longer) laser. This comparison provides evidence of the relative importance of current and carrier density for the degradation process. Despite the higher current density which was comparable to the operating current density of the 2 mm laser, the degradation rate increased much more in the shorter laser. This suggests that the degradation is much more affected by the carrier density required to reach threshold.

A significant result arising from this study is the apparent shift in emission wavelength which occurs with aging. For lasers of all cavity lengths, the emission wavelength measured at 21°C heat-sink temperature and 10% above threshold current was observed to blue-shift, despite an expectation that the active temperature would become higher due to joule heating as the device became less efficient, i.e., an increase in the active region temperature would result in a red-shift, due to the temperature dependence

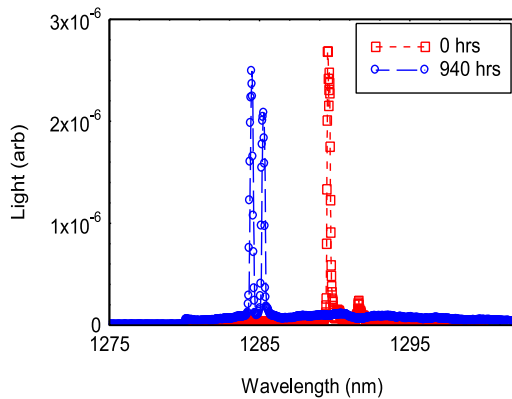


Fig. 4. Emission wavelength for 2 mm laser measure at 20 C and 10% above threshold current before and after reliability testing for total duration of 940 hrs.

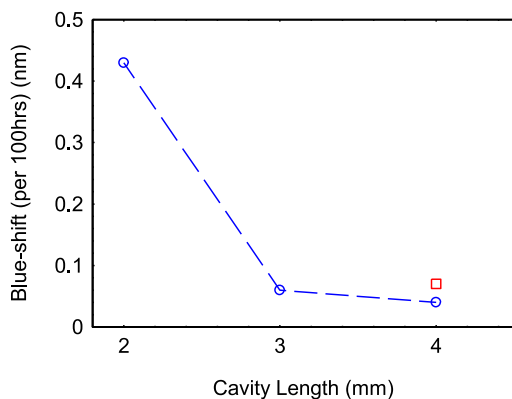


Fig. 5. Shift in emission wavelength, per 100 hrs of operation at 21 °C, plotted as a function of cavity length. Red square data point is for a laser device tested at 3.0 times threshold.

of the band-gap. In the previous study we observed that a longer laser wavelength was measured for samples containing a smaller defect density [7]. An example of the emission wavelength at 10% above threshold for a 2 mm long laser is shown in Fig. 4. The result is consistent with an increase in optical loss, due to an increased presence of defects, that for a given level of current injection reduces the magnitude of the net-gain. To recover the gain to a value which matches the increased loss imposed by the cavity, there must be an increase in the level of injected carriers, which causes an increase in threshold current and via the effect of state-filling, causes a blue-shift of the emission wavelength. As stated above, this effect can be enough to overcome the red-shift of the band-gap induced by increased heating (resulting from the decrease in efficiency as aging proceeds). Note that in Fig. 4, there are two dominant peaks in the blue-shifted spectrum and this is believed to result from competing modes, which are supported by the relatively broad gain spectrum and is not a direct result of the effects of degradation. The extent of the blue-shift appears to be dependent on the cavity length, the shorter the cavity and the greater the degradation the larger the blue-shift, and this is illustrated in Fig. 5. The shift observed when measured at 10% above threshold current for the 4 mm device aged at 3.0 times the initial threshold is also plotted and shows an increase in the blue-shift compared to a 4 mm device degraded

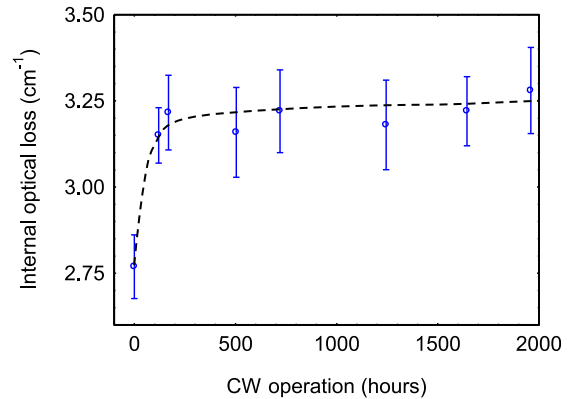


Fig. 6. Measured optical loss before and after CW operation for a 3 mm long laser and the corresponding threshold current density vs. operation time.

at 1.3 times the initial threshold. This is consistent with the observation that the higher operating current density resulted in a larger increase in threshold current density with aging, but not as large as that for the 2 mm long laser. This blue-shift follows from the increase in loss and the increased state-filling required to recover the gain magnitude. It will vary depending on the rate of degradation and the extent of inhomogeneous broadening of the ground state energy distribution. For the samples under test, we did not observe any switch to the excited state, which is typically separated from the ground state by 70–80 nm.

Any increase in optical loss due to degradation will cause an increase in the carrier density required to reach threshold which, if causing significant population of the 2-dimensional states of the system, would reduce the benefits of carrier localisation afforded by the dots and cause further, and ultimately, runaway degradation as seen for the 2 mm long device.

To directly measure the optical loss during the degradation of the QD ridge-waveguide lasers and to determine the origin of this optical loss, we utilise the segmented-contact structure that can also be operated as a laser. Measurements of the internal optical mode loss before and at intervals through the aging process are shown in Fig. 6. This demonstrates that the increase in threshold current density with time occurring during initial rapid degradation is due to an increase in the internal optical mode loss. It is known that internal optical mode loss can increase in the presence of threading dislocations due to the effect of the localised electric field generated by dangling bonds on the local confined state energies [21]. We believe that in the initial stages of degradation there is a relatively large initial increase in the internal optical loss due to dislocation climb. This effect either initiates a run-away process of increased non-radiative recombination and REDR if the increase in loss is large enough to cause substantial population of the 2D states, or stops or slows if no significant rise in non-radiative recombination occurs due to continuing effective confinement of carriers within the dots. We note that none of the degraded samples visibly exhibited any signs of facet degradation when examined under an optical microscope, or by inspection of the nearfield. We also performed the same experiment for samples grown on GaAs substrates (operated under the same conditions) and no degradation in

threshold current density or increase in optical loss was observed over the test period. The sample grown on GaAs had a lower internal optical loss and threshold current density than the Si sample, but the forward bias IV characteristics were similar for both substrate types. The reverse bias leakage current of a typical Si sample is around 45 nA at -2 V, 9 times higher than that for a GaAs sample, and the reverse leakage current has previously been shown to increase with increasing degradation for direct growth on Si [12].

IV. CONCLUSION

InAs QD ridge-waveguide lasers grown directly on Si substrates have been tested for reliability by operating at constant current and taking interval measurements of L-I-V characteristics to determine changes in threshold current and slope efficiency. The rate of degradation depended on the cavity length of the laser being tested, revealing that the longer the laser, and hence the lower the operating carrier density, the lower the rate of degradation. In addition, the operating wavelength of all lasers tested was found to blue-shift as aging proceeded and was greater for lasers with a higher degradation rate indicating that optical loss increased causing an increase in the required threshold carrier density at threshold. No sign of degradation of the facets was observed and measurements of the optical loss taken on a test structure that was aged as a laser and then tested at intervals showed that the internal optical mode loss did increase with aging for the samples grown on silicon. We conclude that even in samples where carriers are localised in the dots and cannot move to defect centres, degradation can still occur through changes in the internal optical mode loss and that the change in threshold carrier density that this causes can lead to population of the extended states of the dot / wetting layer system leading to rapid failure of the devices. In order to minimise degradation we suggest that devices should be operated with the lowest possible carrier density by minimising the optical loss and therefore threshold requirement so that even degradation enhanced changes on internal optical mode loss do not lead to a critical increase in carrier density at threshold.

ACKNOWLEDGMENT

Information on the data underpinning the results presented here can be found in the Cardiff University data catalogue at <http://doi.org/10.17035/d.2019.0075792682>.

REFERENCES

- [1] Z. Mi, J. Yang, P. Bhattacharya, G. Qin, and Z. Ma, "High-performance quantum dot lasers and integrated optoelectronics on Si," *Proc. IEEE*, vol. 97, no. 7, pp. 1239–1249, Jul. 2009.
- [2] S. Chen *et al.*, "Electrically pumped continuous-wave III-V quantum dot lasers on silicon," *Nature Photon.*, vol. 10, no. 5, pp. 307–311, 2016.
- [3] Y. Wan *et al.*, "Sub-wavelength InAs quantum dot micro-disk lasers epitaxially grown on exact Si (001) substrates," *Appl. Phys. Lett.*, vol. 108, no. 22, 2016, Art. no. 221101.
- [4] K. Volz *et al.*, "GaP-nucleation on exact Si (0 0 1) substrates for III/V device integration," *J. Cryst. Growth*, vol. 315, no. 1, pp. 37–47, 2011.
- [5] A. Y. Liu *et al.*, "Electrically pumped continuous-wave 1.3 μm quantum-dot lasers epitaxially grown on on-axis (001) GaP/Si," *Opt. Lett.*, vol. 42, no. 2, pp. 338–341, 2017.

- [6] T. Ward *et al.*, "Design rules for dislocation filters," *J. Appl. Phys.*, vol. 116, no. 6, 2014, Art. no. 063508.
- [7] J. R. Orchard *et al.*, "In situ annealing enhancement of the optical properties and laser device performance of InAs quantum dots grown on Si substrates," *Opt. Express*, vol. 24, no. 6, pp. 6196–6202, 2016.
- [8] J. Norman *et al.*, "Electrically pumped continuous wave quantum dot lasers epitaxially grown on patterned, on-axis (001) Si," *Opt. Express*, vol. 25, no. 4, pp. 3927–3934, 2017.
- [9] D. Inoue *et al.*, "Directly modulated 1.3 μm quantum dot lasers epitaxially grown on silicon," *Opt. Express*, vol. 26, no. 6, pp. 7022–7033, 2018.
- [10] J. Kwoen, B. Jang, K. Watanabe, and Y. Arakawa, "High-temperature continuous-wave operation of directly grown InAs/GaAs quantum dot lasers on on-axis Si (001)," *Opt. Express*, vol. 27, no. 3, pp. 2681–3688, 2019.
- [11] S. Zhu, B. Shi, Q. Li, and K. M. Lau, "1.5 μm quantum-dot diode lasers directly grown on CMOS-standard (001) silicon," *Appl. Phys. Lett.*, vol. 113, no. 22, 2018, Art. no. 221103.
- [12] A. Y. Liu *et al.*, "Reliability of InAs/GaAs quantum dot lasers epitaxially grown on silicon," *IEEE J. Sel. Topics Quantum Electron.*, vol. 21, no. 6, Nov./Dec. 2015, Art. no. 1900708.
- [13] D. Jung *et al.*, "Highly reliable low-threshold InAs quantum dot lasers on on-axis (001) Si with 87% injection efficiency," *ACS Photon.*, vol. 5, no. 3, pp. 1094–1100, 2018.
- [14] Z. I. Kazi, P. Thilakan, T. Egawa, M. Umeno, and T. Jimbo, "Realization of GaAs/AlGaAs lasers on Si substrates using epitaxial lateral overgrowth by metalorganic chemical vapor deposition," *Jpn. J. Appl. Phys.*, vol. 40, no. 8, pp. 4903–4906, 2001.
- [15] P. Petroff and R. L. Hartman, "Defect structure introduced during operation of heterojunction GaAs lasers," *Appl. Phys. Lett.*, vol. 23, no. 8, pp. 469–471, 1973.
- [16] J. P. van der Ziel, R. D. Dupuis, R. A. Logan, and C. J. Pinzone, "Degradation of GaAs lasers grown by metalorganic chemical vapor deposition on Si substrates," *Appl. Phys. Lett.*, vol. 51, pp. 89–91, 1987.
- [17] D. Naidu, P. M. Smowton, and H. D. Summers, "The measured dependence of the lateral ambipolar diffusion length on carrier injection-level in Stranski-Krastanov quantum dot devices," *J. Appl. Phys.*, vol. 108, no. 4, 2010, Art. no. 043108.
- [18] D. Jung *et al.*, "Impact of threading dislocation density on the lifetime of InAs quantum dot lasers on Si," *Appl. Phys. Lett.*, vol. 112, no. 15, 2018, Art. no. 153507.
- [19] P. M. Smowton, I. C. Sandall, H. Y. Liu, and M. Hopkinson, "Gain in p-doped quantum dot lasers," *J. Appl. Phys.*, vol. 101, no. 1, 2007, Art. no. 4181.
- [20] P. Blood *et al.*, "Characterization of semiconductor laser gain media by the segmented contact method," *IEEE J. Sel. Topics Quantum Electron.*, vol. 9, no. 5, pp. 1275–1282, Sep./Oct. 2003.
- [21] H. Iber, E. Peiner, and A. Schlachetzki, "The effect of dislocations on the optical absorption of heteroepitaxial InP and GaAs on Si," *J. Appl. Phys.*, vol. 79, no. 12, pp. 9273–9277, 1996.

Samuel Shutts received the M.Phys. degree from Cardiff University, Cardiff, U.K., in 2008, and the Ph.D. degree in 2013. He has worked as a Research Associate specializing in the design, fabrication, and advanced characterization of III-V semiconductor quantum dot and quantum well lasers. He is currently working as a Research Fellow. He is involved in Innovate U.K. projects for telecom lasers and vertical cavity surface emitting lasers (VCSELs) for miniature atomic clocks, and carries out research for the EPSRC Future Compound Semiconductor Manufacturing Hub.

Craig P. Allford received the B.Sc. degree in theoretical and computational physics from Cardiff University, Cardiff, U.K., in 2009, and the Ph.D. degree in 2016. He was a Postdoctoral Research Associate with Cardiff University in 2016. In 2017, he was working as a Postdoctoral Research Fellow in quantum device characterization with the University of Warwick. In 2018, he was working as a Postdoctoral Research Associate with Cardiff University. His research interests include advanced electrical and optical characterization, and long-term degradation studies of compound semiconductor optoelectronic devices.

Clemens Spinnler received the B.Sc. degree in nanoscience and the master's degree majoring in physics from the University of Basel, Basel, Switzerland. He is currently working toward the Ph.D. degree in nanophotonic with the University of Basel. He was with ETH, Swiss Federal Institute of Technology, Zurich, during his B.Sc. degree and during his master's conducted research in Cardiff University from January to July 2017.

Zhibo Li received B.Eng. degree in electronic engineering from the University of Electronic Science and Technology of China, Chengdu, China, in 2011, and the Ph.D. degree in nanophonics from the University of Glasgow, Glasgow, U.K., in 2015. After graduation, he joined the Key Laboratory of Semiconductor Materials Science, Institute of Semiconductors, Chinese Academy of Sciences, Beijing, China, as a Postdoctoral Researcher to develop the technology of III–V nanolasers growth on silicon. He also worked at DTU Nanolab, Technical University of Denmark as a Visiting Researcher to establish silicon-on-insulator batch processing techniques in 2016. He is currently a Research Associate with the EPSRC Future Compound Semiconductor Manufacturing Hub, School of Physics and Astronomy, Cardiff University, Cardiff, U.K. He has more than eight years of experience in semiconductor processing for a variety of devices covering nanophonics, optoelectronics, and silicon photonics. He is currently working on several projects on design, fabrication, and characterization of III–V quantum dots lasers for telecommunication and sensing applications.

Angela Sobiesierski received the Ph.D. degree in 1997 initially at Swansea University, Swansea, U.K. (1997–2000) and most recently (2000 onward) at Cardiff University, Cardiff, U.K. She worked briefly for DERA Farnborough before working as a Postdoctoral Research Associate. In September 2012, She became a Manager of the cleanroom facility shared between physics and engineering.

Mingchu Tang received the B.Eng. degree in electronic and electrical engineering from the University of Sussex, Brighton, U.K., in 2011, and the M.Sc. degree in nanotechnology from University College London, London, U.K., in 2012. In 2016 he received the Ph.D. degree, working on molecular on molecular beam epitaxy of III–V compound semiconductors and optoelectronic devices with the Photonics group, University College London. His research interests include III–V quantum dot optoelectronic devices monolithically grown on groups III–V and IV platform.

Huiyun Liu received the Ph.D. degree from the Institute of Semiconductor, Chinese Academy of Sciences, Beijing, China. After receiving the Ph.D. degree, he joined the EPSRC National Centre for III–V Technologies with the University of Sheffield, Sheffield, U.K., in August 2001. He was responsible for the development of molecular beam epitaxy growth of semiconductor materials for the U.K. academic and industrial research community. In 2007, he received Royal Society University Research Fellow Award and started his academic career with the Department of Electronic and Electrical Engineering, University College London, London, U.K., as a Senior Lecturer. In 2012, he was promoted to the Chair for the Semiconductor Photonics.

Peter M. Smowton received the B.Sc. degree in physics and electronics and the Ph.D. degree in electrical engineering from the University of Wales, Cardiff, U.K., in 1987 and 1991, respectively. He is the Director of the EPSRC Future Compound Semiconductor Manufacturing Hub, which is a U.K. multi-university research project focused on the manufacturing processes for the Compound Semiconductor materials and devices that drive much of the technology that underpins our lives. He is currently the Managing Director of the Institute of Compound Semiconductors, which is a University translational research facility focused on the fabrication of compound semiconductor devices and integrated systems. He is a Professor of optoelectronic device physics and the Head of the School of Physics and Astronomy with Cardiff University, Cardiff, U.K. He is also a Director of the Compound Semiconductor Centre, Cardiff.